Non-Coherent Near-Capacity Network Coding for Cooperative Multi-User Communications

Hung Viet Nguyen, Chao Xu, Soon Xin Ng, *Senior Member, IEEE*, and Lajos Hanzo, *Fellow, IEEE*

***Abstract*—Near-capacity Non-coherent Cooperative Network-coding aided Multi-user (NNCNM) systems are designed with the aid of Extrinsic Information Transfer (EXIT) charts for the sake of approaching the Differential Discrete-input Continuous-output Memoryless Channel's (D-DCMC) system capacity[1]. The upper and lower Frame Error Ratio (FER) performance bounds are derived for aiding our network coding design. The outage capacity of the D-DCMC channel is also calculated and used for computing the best-case performance bounds of both the corresponding single-link scheme and of the proposed NNCNM system. Moreover, a new technique referred to as the Pragmatic Algebraic Linear Equation Method (PALEM) was proposed for determining the exact number of information sources that may be recovered from the composite NNCNM stream, which constitutes a lower-complexity evaluation of the attainable FER performance of the NNCNM systems without resorting to high-complexity Monte-Carlo simulations. The NNCNM systems advocated are capable of operating within 0.3-0.5 dB from the corresponding D-DCMC capacity. A joint treatment of channel and network coding is considered in our system[2]. The design principles presented in this contribution may be extended to a vast range of NNCNM based systems using arbitrary channel coding schemes.**

***Index Terms*—Differential detection, channel coding, network coding and cooperative communications.**

I. INTRODUCTION

NETWORK coding has been shown to be capable of increasing the achievable throughput, while minimising both the amount of energy as well as delay of packets travelling through the network [2]–[5]. Dynamic Network Codes (DNC) were proposed by Xiao et al. [5]–[8], where each of the M users broadcasts a single Information Frame (IF) of its own both to the Base Station (BS) and to the other users during the first Time Slot (TS). Then, during the 2^{nd} to the $(M)^{th}$ TS, each user transmits to the BS $(M-1)$ nonbinary linear combinations of those particular IFs that were successfully decoded.

Generalised Dynamic Network Codes (GDNC) were proposed in [9], [10] by interpreting the design problem as being equivalent to that of designing linear block codes defined over GF(q) for erasure correction. The authors of [9], [10] extended the original Dynamic Network Code (DNC) concept presented in [6]–[8] by allowing each user to broadcast several (as opposed to a single in [6]–[8]) IFs of its own during the broadcast phase (BP) via orthogonal channels, as well as to transmit several nonbinary linear combinations, which are also considered as Parity Frames (PFs), during the Cooperative Phase (CP) via orthogonal channels. The FER performance of the GDNC scheme was determined in [9] by calculating the rank of the matrix characterising GDNCs. This method, which we refer to as the Purely Rank-Based Method (PRBM), always provides an optimistic estimate of the attainable FER performance of GDNCs.

Tüchler and Hagenauer proposed the employment of Irregular Convolutional Codes (IrCCs) [11], [12] for serially concatenated schemes, which are constituted by a family of convolutional codes having different rates, in order to design a near-capacity system. They were specifically designed with the aid of Extrinsic Information Transfer (EXIT) charts conceived for analysing the convergence properties of iterative decoding aided concatenated coding schemes [13].

As the number of sources and relays increases, it becomes unrealistic to obtain accurate Channel State Information (CSI) for the increasing number of mobile-to-mobile channels. As a result, the CSI-errors may erode the performance of the near-capacity coherent modulation schemes designed with the aid of EXIT charts relying on the assumption of perfect CSI estimation. Hence Differential M-ary Phase-Shift Keying (DMPSK) can be chosen for the sake of eliminating the excessive complexity of channel estimation in distributed networks [14].

Furthermore, Multiple-Symbol Differential Detection (MSDD) [15] may be employed in order to mitigate the performance loss of the non-coherent receivers. Since the differential encoder is 'recursive' – i.e. has an infinite impulse response – similar to Recursive Systematic Convolutional (RSC) codes, the (1,1) point of the EXIT chart can be approached by MSDD having a detection window length as long as the decoding frame length. However, the computationally affordable MSDD window length is severely limited, because its extension imposes an exponentially increasing detection complexity. As a remedy, Multiple-Symbol Differential Sphere Detection (MSDSD) [16] was proposed for reducing the complexity, but the employment of a frame-sized detection window length still remains impractical. Furthermore, having a slightly degraded performance is unavoidable, since MSDSD constitutes the

Paper approved by E. Ayanoglu, the Editor for Communication Theory and Coding Applications of the IEEE Communications Society. Manuscript received August 15, 2011; revised January 6 and March 12, 2012.

The authors are with the School of ECS, University of Southampton, SO17 1BJ, UK (e-mail: {hvn08r, cx1g08, sxn, lh}@ecs.soton.ac.uk).

The financial support of the Vietnamese International Education Development (VIED) fund and the EU under the auspices of the CONCERTO project as well as of the RC-UK under the India-UK Advanced Technology Centre is gratefully acknowledged.

Digital Object Identifier 10.1109/TCOMM.2012.071912.110540

[1]Part of this work was presented at VTC2011-Fall [1].

[2]The authors are grateful to the anonymous reviewer for the suggestion of conceiving combined non-coherent network coding and detection in their future work.

Max-Log-MAP – rather than MAP – algorithm [17] of MSDD. Therefore, a recursive Unity-Rate Code (URC) [18] having an infinite impulse response may be employed as an intermediate code. In other words, a near-capacity channel coding scheme - namely IrCC-URC-DMPSK associated with MSDD - can be invoked for the sake of approaching the achievable non-coherent-detection based channel capacity, while the high-complexity, yet imperfect channel estimation requiring a high pilot-overhead is eliminated.

Additionally, implementing iterative decoding exchanging extrinsic information between channel coding and network coding is capable of improving the system's performance. This idea has been studied in [19], [20]. However, extending our knowledge acquired from [19], [20] to iterative decoding in the context of our scenario considering multiple-relays/users[3] leads to an extremely high complexity, rendering the adoption of a joint channel-network code design impractical. This conclusion was also suggested by Iscan and Hausl in [21]. Alternatively, the inter-operation of channel-and network-coding may be exploited to provide an improved performance, as suggested in [22]. We further develop this philosophy for the case of employing a practical rather than an ideal/perfect channel code.

Against this background, the novel contribution of this article is that a practical near-capacity channel coding scheme is designed with the aid of EXIT charts for the sake of supporting non-coherent cooperative communications. The design guidelines presented in this contribution can also be extended to a diverse range of other network-coding aided multiuser systems employing arbitrary channel coding schemes. More specifically:

1) The near-capacity coded differential modulation scheme associated with MSDD is then employed in the proposed network-coding based system, in order to achieve a good performance in the absence of channel estimation. The near-capacity coded differential modulation scheme associated with MSDD is designed with the aid of EXIT charts under the consideration of the effects of both the shadow-fading and of the small-scale Rayleigh fading in our channel model.
2) We introduced and formulated the complementary Cumulative Distribution Function (CDF) $F(SNR_r|_R)$ for characterising the D-DCMC channel employing MSDD aided DMPSK. This CDF function has been computed with the aid of EXIT charts. Based on $F(SNR_r|_R)$, we defined and formulated the outage capacity of the differentially encoded modulation scheme corresponding to different outage probability values ε. This outage capacity is employed for computing the best-case performance bounds of both the single-link scheme and of the Non-coherent Cooperative Network-coding aided Multi-user (NNCNM) system.
3) Based on the upper bound and lower bound formulae conceived for a coherent Continuous-input Continuous-output Memoryless Channel (CCMC) based network coding aided system in [4], we further extend these formulae for calculating the FER performance bounds and for the diversity order of the NNCNM system. These bounds guide our network coding design as well as assist us in estimating the FER performance of the NNCNM system without running extremely time-consuming Monte-Carlo simulations.
4) Based on the algorithms employed for recovering the transmitted frames at the base station (BS), we proposed a new method that we refer to as the Pragmatic Algebraic Linear Equation Method (PALEM). This method is capable of accurately characterising the system's FER performance. The system's performance estimated by the PALEM is compared to that obtained by the PRBM.
5) The idea of adaptive network coding suggested in [22] is also considered in our system for the joint treatment of channel-network coding in order to improve the multiplexing capability of the network coding scheme used in our system.

The rest of this article is organised as follows. In Section II, outage probabilities are derived before highlighting the MSDD-aided-DMPSK scheme's architecture. Then, our system model is portrayed and the detector employed at the BS is detailed, along with the portrayal of the proposed method PALEM. The bounds of the system's outage probability are derived in Section III. Then, the system parameters are summarised in Section IV. In Section V, we propose appropriate design procedures for both our near-capacity IrCC-URC-MSDD-aided-DMPSK arrangement and for network coding. Furthermore, we conceive an EXIT-chart based method for computing the D-DCMC outage capacity. Our performance results are discussed in Section VI, before offering our conclusions in Section VII.

II. Preliminaries

A. Single Link Channel Outage Probability

We consider a single transmission link associated with the transmitted and received signals of x and y, respectively. The received signal can be represented as

$$y = hx + n \ , \tag{1}$$

where $h = h_s h_f$ is the complex-valued fading coefficient comprised of two components, a slow fading coefficient (large-scale shadow fading or quasi-static fading) h_s, which is constant for all symbols within a transmission frame and a fast fading (small-scale Rayleigh fading) coefficient h_f, which varies on a symbol by symbol basis, while n is the Additive White Gaussian Noise (AWGN) process having a variance of $N_0/2$ per dimension.

We refer to C as the maximum achievable transmission rate of reliable communication supported by this channel. Let us assume that the transmitter encodes data at a rate of R bits/s/Hz. If the channel realisation h has a capacity of $C|_h < R$, the system is declared to be in outage, where the outage probability is given by:

$$P_e(R) = Pr\left\{C|_h < R\right\} \ , \tag{2}$$

and $C|_h$ is the capacity, i.e. the maximum achievable rate of the channel, provided that h is known. If x is i.i.d.,

[3]In our scenario, each user itself plays a role as a relay. Hence, our model has multiple-users and multiple-relays.

the transmission link obeys the CCMC model. The outage probability for the CCMC channel is given by [23]

$$P_e^{CCMC}(R) \;=\; Pr\left\{|h_s|^2\mathrm{E}\left[|h_f|^2\right] < \frac{2^R-1}{SNR}\right\}, \quad (3)$$

where $SNR = \frac{E[|X|^2]}{N_0} = \frac{1}{N_0}$ is the signal to noise power ratio, when $E[|X|^2] = 1$.

We define the receiver's SNR as $SNR_r = E[|h|^2 SNR] = |h_s|^2/N_0$ when $E[|h_f|^2] = 1$, and consider a D-DCMC having a data rate of $R = \eta R_c$, where η is the number of modulated bits and R_c is the equivalent channel coding rate. At a given data rate R, we can identify the corresponding $SNR_r|_R$ point on the D-DCMC capacity curve, which will be calculated by using EXIT-charts in Section V-A. Then, similar to (3), the outage probability of the D-DCMC model is equivalent to the probability of the specific event that we have $|h|^2 SNR < SNR_r|_R$:

$$P_e^{D-DCMC}(R,\eta) = Pr\left\{|h_s|^2\mathrm{E}[|h_f|^2] < \frac{SNR_r|_R}{SNR}\right\}. \quad (4)$$

B. MSDD-aided-DMPSK

For DMPSK schemes, differential encoding is carried out according to:

$$s_n = \begin{cases} s_1 & n = 1 \\ x_{n-1}s_{n-1} & n > 1 \end{cases}, \quad (5)$$

where x_n carries the source information. For a single transmission link, the signal received over a Rayleigh fading channel may be expressed as:

$$y_n = s_n h_n + n_n, \quad (6)$$

where the AWGN n_n has a zero mean and a variance of N_0, while h_n denotes the fading coefficient having a temporal correlation of $\varepsilon\{h_n h_{n+k}^*\} = J_0(2\pi k f_d)$ according to Clarke's fading model mentioned in [15], where J_0 denotes the zero-order Bessel function of the first kind and f_d is the normalized Doppler frequency.

In order to observe the received signal across an MSDD decision window of N_w consecutive symbols, (6) may be further developed as:

$$\mathbf{y} = \mathbf{s}\mathbf{h} + \mathbf{n}, \quad (7)$$

where the $(N_w \times 1)$-element matrix $\mathbf{y} = [y_{n-N_w+1}, \cdots, y_n]^T$ models the received symbols within the MSDD window, while the equivalent fading channel matrix $\mathbf{h} = [h_{n-N_w+1}, \cdots, h_n]^T$ and the equivalent AWGN matrix $\mathbf{n} = [n_{n-N_w+1}, \cdots, n_n]^T$ are both of size $(N_w \times 1)$. The $(N_w \times N_w)$-element equivalent transmission matrix $\mathbf{s}$ of (7) is modelled as $\mathbf{s} = \mathrm{diag}\{[s_{n-N_w+1}, \cdots, s_n]\}^T$.

The MSDD aims for minimizing the *a posteriori* probability of [15]:

$$\Pr(\mathbf{y} \mid \mathbf{s}) = \frac{\exp\left[-\mathrm{tr}\left\{\mathbf{y}^H(\mathbf{R_{yy}})^{-1}\mathbf{y}\right\}\right]}{\pi^{N_w}\det(\mathbf{R_{yy}})}, \quad (8)$$

where the correlation matrix $\mathbf{R_{yy}}$, whose determinant is a real-valued constant, is given by:

$$\mathbf{R_{yy}} = \mathbf{s}\mathbf{R_{hh}}\mathbf{s}^H + \mathbf{R_{nn}} = \mathbf{s}\mathbf{C}\mathbf{s}^H, \quad (9)$$

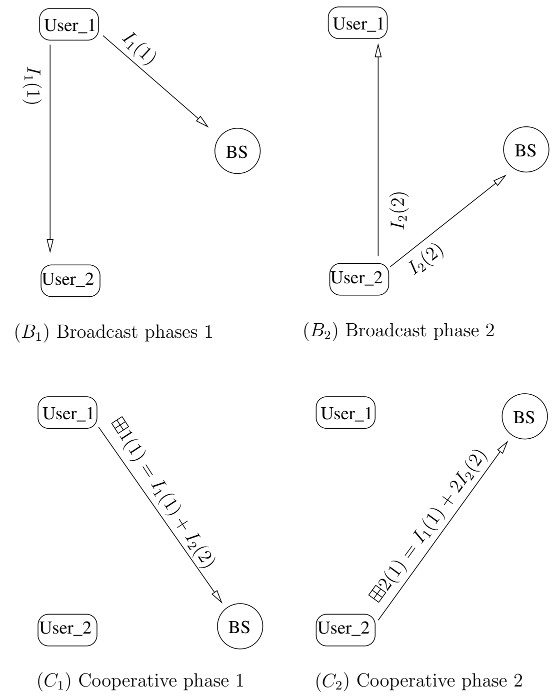

Fig. 2: The model of the system having $M = 2$ users, and each user transmits $k_1 = 1$ information frames and $k_2 = 1$ parity frames.

where the correlation of the fading channel is given by $\mathbf{R_{hh}} = \mathrm{Toeplitz}\{\rho_0, \cdots, \rho_{N_w-1}\}$[4], with $\rho_k = NJ_0(2\pi k f_d)$, while the correlation matrix of the AWGN is given by $\mathbf{R_{nn}} = N_0 \cdot \mathbf{I_{N_w}}$. The channel's correlation matrix in (9) is defined as $\mathbf{C} = \mathbf{R_{hh}} + \mathbf{R_{nn}}$. Therefore, the trace operation in (8) may be further formulated as:

$$\mathrm{tr}\left\{\mathbf{y}^H(\mathbf{R_{yy}})^{-1}\mathbf{y}\right\} = \mathrm{tr}\left\{\mathbf{y}^H\mathbf{s}\mathbf{C}^{-1}\mathbf{s}^H\mathbf{y}\right\} = \left\|\mathbf{L}^H\mathbf{s}^H\mathbf{y}\right\|^2, \quad (10)$$

where the lower triangular matrix $\mathbf{L}$ is generated by the decomposition of $\mathbf{C}^{-1} = \mathbf{L}\mathbf{L}^H$. Based on the *a posteriori* probability of (8), the Log-MAP algorithm conceived for MSDD-aided-DMPSK may be formulated as (11) where $L_e(b_k \mid \mathbf{y})$ denotes the extrinsic LLR provided for the bit b_k, while $\mathbf{s}_0^k$ and $\mathbf{s}_1^k$ refer to the constellation set corresponding to the equivalent transmission matrix $\mathbf{s}$ when b_k is set to 0 and 1, respectively.

C. System Model

The system's general architecture may be structured into two layers, namely channel coding and network coding, as seen in Fig 1. Let us initially portray the network coding aspect by describing a simple system, which is illustrated in Fig 2. This system has $M = 2$ users communicating with a BS [6], where a transmission session consists of $(k_1 M + k_2 M) = 4$ phases, namely the BPs B_1 and B_2, as well as the CPs C_1 and C_2. For simplicity, we refer to a single transmission phase (BP or CP) as a time slot, in which a user transmits a single frame (IF or PF).

[4]This notation simply indicates that R_{hh} is a Toeplitz-structured matrix constituted by the elements $\{\rho_0, \cdots, \rho_{N_w-1}\}$

$$L_e(b_k \mid \mathbf{y}) = \ln\left(\frac{\sum_{\mathbf{s}\in\mathbf{s}_1^k} \exp\left[\left\|\mathbf{L}^H\mathbf{s}^H\mathbf{y}\right\|^2 + \sum_{j=1,j\neq k}^{N_w(\log_2 M)} b_j L_a(b_j)\right]}{\sum_{\mathbf{s}\in\mathbf{s}_0^k} \exp\left[\left\|\mathbf{L}^H\mathbf{s}^H\mathbf{y}\right\|^2 + \sum_{i=1,i\neq k}^{N_w(\log_2 M)} b_i L_a(b_i)\right]}\right), \quad (11)$$

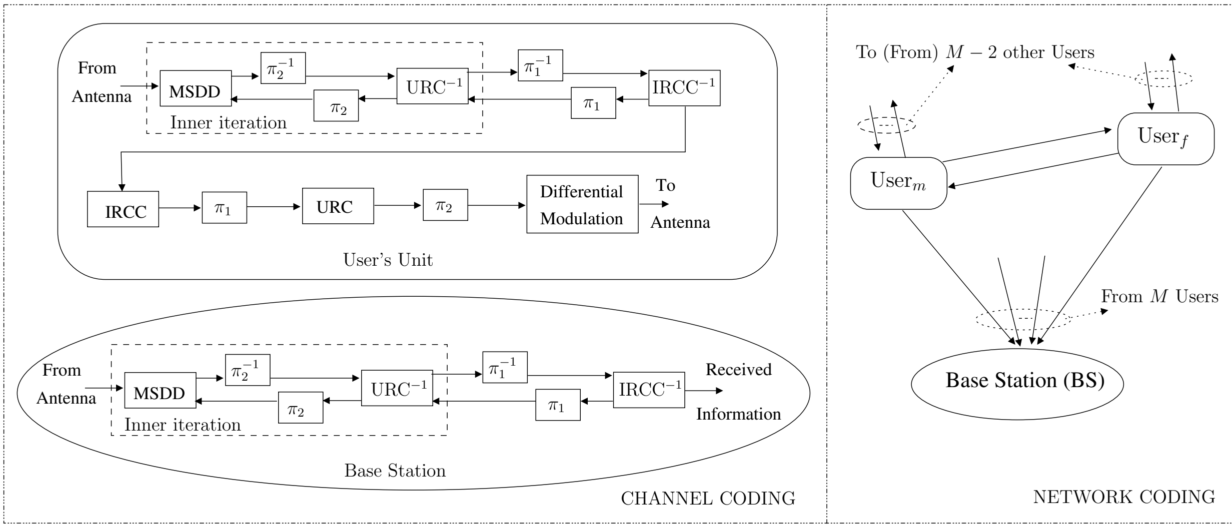

Fig. 1: The system general architecture.

As seen in Fig 2, each user participating in the transmission session transmits $k_1 = 1$ IF during the corresponding BP and $k_2 = 1$ PF during the corresponding CP according to the transfer matrix $\boldsymbol{G}_{2\times 4}$ [6]–[8]

$$\boldsymbol{G}_{2\times 4} = \left[\begin{array}{cc|cc} 1 & 0 & 1 & 1 \\ 0 & 1 & 1 & 2 \end{array}\right], \quad (12)$$

where the PF transmitted by User 1 (or User 2) during the CP C_1 (or C_2) is given by $\boxplus 1(1) = \boldsymbol{G}_{2\times 4}(1,3)I_1(1) + \boldsymbol{G}_{2\times 4}(2,3)I_2(2) = I_1(1) + I_2(2)$ (or $\boxplus 2(1) = \boldsymbol{G}_{2\times 4}(1,4)I_1(1) + \boldsymbol{G}_{2\times 4}(2,4)I_2(2) = I_1(1) + 2I_2(2)$)[5]. The variable $I_i(i)$, $i = [1,2]$, represents the IF transmitted by User i during the BP B_i, while the variable $\boxplus i(j)$ represents the j^{th} PF of User i.

We then define $\boldsymbol{G}'_{2\times 4}$ as the corresponding *modified* transfer matrix, where the terminology *modified* implies that the entries of $\boldsymbol{G}'_{2\times 4}$ are modified with respect to those of the original transfer matrix $\boldsymbol{G}_{2\times 4}$ of (12) according to the success/failure of each transmission phase within an actual transmission session. The further detailed mathematical description of the modified matrix $\boldsymbol{G}'_{2\times 4}$ can be found in [4].

Let us now generalise the network coding model of Fig 1. The transfer matrix $\boldsymbol{G}_{k_1M\times k_1M+k_2M}$ (or $\boldsymbol{G}$ for shorthand) comprising the identity matrix $\boldsymbol{I}_{k_1M\times k_1M}$ (or $\boldsymbol{I}$ for shorthand) and the parity matrix $\boldsymbol{P}_{k_1M\times k_2M}$ (or $\boldsymbol{P}$ for shorthand) represents a transmission session of the system, where all the frames transmitted during that session are successfully decoded. We also define the modified transfer matrix $\boldsymbol{G}'_{k_1M\times k_1M+k_2M}$ (or $\boldsymbol{G}'$ for shorthand) representing an actual transmission session. Note that the corresponding identity matrix $\boldsymbol{I}'$ of matrix $\boldsymbol{G}'$ represents the results of the transmissions of the Mk_1 IFs transmitted from the M users to the BS during the k_1M broadcast phases. By contrast, the corresponding parity matrix $\boldsymbol{P}'$ of matrix $\boldsymbol{G}'$ illustrates the results of all the inter-user transmissions during the k_1M broadcast phases as well as the transmission results of all PFs transmitted from the M users to the BS during the k_2M cooperative phases. The formation of the matrices $\boldsymbol{G}$ and $\boldsymbol{G}'$ is detailed in [4].

When considering the channel coding aspects, we assume that all the links in the system are supported by channels having the same information rate R. In order to achieve an infinitesimally low BER, turbo detection may be employed at both the User's unit and the BS. Similar to the classic Recursive Systematic Convolutional (RSC) codes, the differential encoder of the DPSK has a recursive structure, i.e. an infinite-duration impulse response, which efficiently spreads the extrinsic information during iterative detection. Hence, theoretically a free distance of $d = 2$ may be achieved by a combined RSC decoder and a MSDD having a detection window size, which has to be as long as the encoding frame length. However, the computationally affordable MSDD window length is severely limited, because its extension imposes an exponentially increasing detection complexity. As a remedy, MSDSD [16] was proposed for reducing the complexity, but the employment of a frame-sized detection window length still remains impractical. In addition, having a slightly degraded performance is inevitable, since MSDSD constitutes the Max-Log-MAP – rather than MAP – algorithm [17] of MSDD. Therefore, a recursive URC [18] having an infinite impulse response may be employed as an intermediate code, as seen in the channel coding section of Fig 1. If the User's unit and the BS can afford the IRCC decoding complexity, then a near-capacity performance may be achieved by employing the three-stage coding arrangement IRCC-URC-DMPSK. In order to exploit the benefits of the turbo principle, two interleavers, namely π_1 and π_2, are employed for efficiently spreading the extrinsic information in support of the inner iterations occurring between the MSDD and the URC decoder, as well

[5]The $\boxplus$ operation in this context was first introduced in [6], [7].

as the outer iterations between the MSDD-URC arrangement and the IRCC decoder.

D. Recovery of the frames at the base station

As the system proceeds through an actual transmission session, the corresponding modified transfer matrix $\boldsymbol{G}^{'}$, which is formed, consists of the identity matrix $\boldsymbol{I}^{'}$ and its parity matrix $\boldsymbol{P}^{'}$. The frames successfully received at the BS can be represented as [4]

$$(a)\ \boldsymbol{X}\boldsymbol{I}^{'} = \boldsymbol{Y}_{I'}, (b)\ \boldsymbol{X}\boldsymbol{P}^{'} = \boldsymbol{Y}_{P'}, \tag{13}$$

where $\boldsymbol{X}$ is a matrix representing the IFs transmitted by the M users during the transmission session of the system, while the matrices $\boldsymbol{Y}_{I'}$ and $\boldsymbol{Y}_{P'}$ represent the frames successfully received at the BS during the BPs and CPs, respectively. In line with [4], [9], [10], we assume that the BS is aware of how each PF was constructed, hence $\boldsymbol{G}'$ is known at the BS. As a result, the BS can certainly recover a set $\boldsymbol{X}_{I'}$ of IFs, which is a subset of $\boldsymbol{X}$, from $\boldsymbol{Y}_{I'}$ as

$$\boldsymbol{X}_{I'} = \boldsymbol{Y}_{I'}. \tag{14}$$

Substituting $\boldsymbol{X}_{I'}$ given by (14) into $(13b)$ we arrive at

$$(\boldsymbol{X} - \boldsymbol{X}_{I'})\boldsymbol{P}^{'} = \boldsymbol{Y}_{P'} - \boldsymbol{X}_{I'}\boldsymbol{P}^{'}. \tag{15}$$

Then, a set $\tilde{\boldsymbol{X}}_{P'}$ of IFs is retrieved from (15) by using the Gaussian elimination algorithm [24]. Ultimately, the entire set of IFs recovered at the BS is $\tilde{\boldsymbol{X}}_{P'} \bigcup \boldsymbol{X}_{I'}$ out of the $\boldsymbol{X}$ of IFs.

It was demonstrated in [4] that the PRBM always produces an optimistic result in comparison to the actual one, which is based on the recovery of the frames based on by (13), (14) and (15).

E. Pragmatic Algebraic Linear Equation Method

Based on the algorithms employed for the recovery of the frames at the BS presented in Section II-D, we proposed a new method that we refer to as the Pragmatic Algebraic Linear Equation Method, which is capable of accurately characterising the system's FER performance. Employing solely the modified transfer matrix $\boldsymbol{G}'$, PALEM facilitates a lower-complexity evaluation of the attainable FER performance of the NNCNM system-family Monte-Carlo simulations. In the PALEM context, the recovery of IFs applied at the BS relies on determining the specific 'variables'[6] that may be retrieved from a set of the linear equations formulated from the modified transfer matrix $\boldsymbol{G}^{'}$. Then, the PALEM can be represented in form of the following three main steps:

1) Specify the rank of the transfer matrix $\boldsymbol{G}$ and $\boldsymbol{I}^{'}$: $\text{rank}(\boldsymbol{G}) = R_F, \text{rank}(\boldsymbol{I}^{'}) = R_{\boldsymbol{I}'}$;
2) Set all the specific variables that can be recovered with the aid of the matrix $\boldsymbol{I}^{'}$ in the entire modified transfer matrix $\boldsymbol{G}^{'}$ to zero for the sake of forming a new transfer matrix $\boldsymbol{G}^{''}$;
3) Let us now denote the number of recoverable variables by N_c, which is a function of R_F, $R_{\boldsymbol{I}'}$, $R_{\boldsymbol{P}''}$ and K_F, where $R_{\boldsymbol{P}''}$ is the rank of the parity matrix $\boldsymbol{P}^{''}$, and K_F is the number of variables that can be recovered with the aid of the matrix $\boldsymbol{P}^{''}$. Note that if the number of variables to be recovered equals to the rank of the matrix established from the corresponding set of the linear equations, then it is possible to recover all the variables. However, if $R_{\boldsymbol{I}'} + R_{\boldsymbol{P}'} < R_F$, we can only recover K_F number of variables from the matrix $\boldsymbol{P}^{''}$. More specifically, the matrix $\boldsymbol{P}^{''}$ can be transformed into an upper triangular transform $\boldsymbol{P}^{''}_{U,T}$ of the transposed matrix $\boldsymbol{P}^{''}$. Then, we can recover $K_F (< R_F - R_{I'})$ number of variables via an iterative detect-and-substitute procedure based on $\boldsymbol{P}^{''}_{U,T}$. Hence, we have

$$N_c = \begin{cases} R_F & : \ R_{\boldsymbol{I}'} + R_{\boldsymbol{P}''} = R_F \\ R_{\boldsymbol{I}'} + K_F & : \ R_{\boldsymbol{I}'} + R_{\boldsymbol{P}''} < R_F \end{cases}. \tag{16}$$

In order to compare the result obtained by the PALEM to that provided by PRBM as well as by Monte-Carlo simulations, let us recall the example of an actual transmission session detailed in [4], which results in the modified transfer matrix $\boldsymbol{G}^{'}_s$ given by

$$\boldsymbol{G}^{'}_s = \left[\begin{array}{cc|cc} 0 & 0 & 0 & 1 \\ 0 & 0 & 0 & 2 \end{array} \right]. \tag{17}$$

In this example, the PRBM of [9] suggests that the number of variables that can be recovered from $\boldsymbol{G}^{'}_s$ would be $N_c = 1$, since the rank of the matrix $\boldsymbol{G}^{'}_s$ is $R_{(\boldsymbol{G}^{'}_s)} = 1$. In reality however, given a linear equation formulated as $1 \times I_1(1) + 2 \times I_2(2) = c_2$, which depends on the pair of variables $I_1(1)$ and $I_2(2)$, it is impossible to retrieve any variable. In contrast to the optimistic decision of the PRBM of $N_c = 1$, the correct result of $N_c = 0$ was obtained by the PALEM as well as by the actual recovery of the frames by employing (13), (14) and (15).

III. Bounds of The System's Outage Probability

Let $U_{m,t}$ be a set of user indices corresponding to the specific users that succeeded in correctly recovering an IF $I_m(t)$ transmitted by User m during TS t. Note that User m itself is always included in this set. Let us denote the number of members in the user set $U_{m,t}$ by $||U_{m,t}||$. Then, the strict upper bound P_o^{Upper} of the system's outage probability P_o may be calculated by [4]:

$$P_o^{Upper} = \Omega + \binom{E+F}{F} \frac{P_e^{M+k_2}(1-P_e)}{1 - P_e - \frac{E}{F+1}P_e} \frac{1-R_o^M}{1-R_o}, \tag{18}$$

where we have $E = (Mk_1 - 1)$, $F = Mk_2$ and $R_0 = (1-P_e)P_e^{k_2-1}$, provided that P_e is the outage probability of the single link as defined in [25], while the term Ω can be determined by

$$\Omega = \left[\binom{k_1 + k_2 - 1}{k_2} - \binom{E+F}{F} \right] \frac{P_e^{M+k_2}(1-P_e)}{1 - P_e - \frac{E}{F+1}P_e}. \tag{19}$$

[6]The variables in this context are defined as the information frames transmitted by all the M users during the broadcast phases. These frames are contained in either the information frames or the parity frames received at the BS.

According to [4], the strict lower bound P_o^{Lower} can be calculated by:

$$P_o^{Lower} = \frac{\binom{E+F}{F} P_e^{F+1} \left[\left(\frac{P_e}{E+F} \right)^{E+1} - (1-P_e)^{E+1} \right]}{(1-P_e)^{1-M} \left(\frac{P_e}{E+F} + P_e - 1 \right)}. \quad (20)$$

IV. The System's Diversity Order and Its Parameters

According to [6]–[10], the diversity order D_{NNCNM} of the system is bounded by

$$M + k_2 \leq D_{NNCNM} \leq Mk_2 + 1. \quad (21)$$

The authors of [6]–[10] inferred the diversity order D_{NNCNM} found in (21) based on the following formula:

$$D_{NNCNM} = \lim_{SNR \to \infty} \frac{-\log_2 P_o}{\log_2 SNR} , \quad (22)$$

where the order of P_e for the best-and worst-case P_o value was estimated and used instead of P_o itself. Furthermore, by exploiting the most influential terms of P_o^{Upper} and P_o^{Lower} instead of P_o itself [4] in (22), it may be seen that the upper- and lower-bounds of the probability P_o are in harmony with the estimated diversity order given by (21).

For notational convenience, we characterise the system by using the set of main parameters $(R, M, k_1, k_2, \boldsymbol{G}, R_{NNCNM}, D_{NNCNM})$, where the system's overall information rate R_{NNCNM} is calculated by:

$$R_{NNCNM} = R_{info} R = \frac{k_1 R}{k_1 + k_2} , \quad (23)$$

provided that the network coding information rate R_{info} is expressed as [9], [10]

$$R_{info} = \frac{k_1}{k_1 + k_2} . \quad (24)$$

We then define E_b/N_0 as the energy per bit to noise power spectral density ratio, which can be computed in our system as:

$$E_b/N_0 = \frac{SNR}{R_{NNCNM}} = SNR \frac{k_1 + k_2}{k_1 R} . \quad (25)$$

To summarise, the main parameters of the system are briefly described in the Table I.

V. Near-Capacity Coding Design

In this section, we first design a powerful channel coding scheme for minimising the probability of errors imposed by link-level transmissions. The details of our design procedure and its performance evaluation are presented in Sections V-A and V-B. Then, based on the number of active users, a suitable transfer matrix is constructed from an appropriately chosen generator matrix of classic Reed Solomon (RS) codes, which are maximum minimum distance codes. The generator matrix of RS codes constructed over the Galois Field GF(q) is provided by the software application SAGE [26]. Again, the parameters characterising the system may be adjusted to meet diverse design criteria, such as the system's effective information rate, or its expected FER-performance estimated on the basis of the system's diversity order, etc. This process is detailed in Section V-C, while in Section V-D, an adaptive mechanism is conceived for improving the system's performance.

A. Near-Capacity Channel Code Design

According to (1) and (3), the average SNR_r per frame can be expressed as

$$SNR_r = \frac{\mathrm{E}[|h_s|^2]\mathrm{E}[|h_f|^2]\mathrm{E}[|x|^2]}{N_0} = \frac{|h_s|^2}{N_0} , \quad (26)$$

where we have $\mathrm{E}[|x|^2] = 1$, $\mathrm{E}[|h_f|^2] = 1$ and $\mathrm{E}[|h_s|^2] = |h_s|^2$ for correlated Rayleigh fading channels. Given a specific SNR_r, we can generate the EXIT chart [13] of the system. As stated in Section I, a near-capacity IrCC-URC-MSDD-aided-DMPSK channel coding scheme is chosen for the sake of approaching the achievable channel capacity. For reasons of simplicity, we present our generic design procedure for the specific example of a specific IrCC-URC-Differential Quadrature Phase Shift Keying (IrCC-URC-DQPSK) design associated with MSDD of $N_w = 4$ using our generically applicable EXIT-chart aided method, which is briefly summarised as follows:

Step1: Create the EXIT curve of the inner decoder component constituted by our URC-MSDD-aided-DQPSK scheme for different SNR_r values;

Step2: We opt for the normalised data rate of $R = \eta \times R_c = 2 \times 0.5$, which is chosen independently from the other parameters of the system. We then fix the IrCC code rate of $R_c = 0.5$, which is also chosen independently from the other parameters of the system, and employ the EXIT curve matching algorithm of [27] for generating the optimised weighting coefficients $\alpha_i, i = 1, ..., 36$, of the 36 different-rate component IrCC codes. More specifically, we opt for the set of codes facilitating decoding convergence to a vanishingly low BER at the lowest possible SNR_r, while ensuring that the Monte-Carlo simulation based decoding trajectory reaches the point of perfect convergence at (1,1) at the top-right corner of the corresponding EXIT chart. This implies that a near-capacity performance can be achieved, as detailed in [28].

Having implemented the design steps mentioned above, we obtain the EXIT curves and the corresponding IrCC component-code weighting coefficients α_i, $i = 1, ..., 36$, as shown in Fig. 3. Again, as detailed in [28], these weighting coefficients α_i determine the particular fraction of the input stream to be encoded by the i^{th} IrCC component code having a code rate of α_i. The EXIT-chart results show that provided a sufficiently high number of iterations, J is carried out between the IrCC decoder and the composite URC-MSDD-aided-DQPSK decoder, the Monte-Carlo simulation based decoding trajectory would reach the $(1, 1)$ point in Fig. 3, which guarantees a vanishingly low BER.

Furthermore, the area property of EXIT-charts [29] states that the area under the EXIT curve of an inner decoder component is approximately equal to the attainable channel capacity, provided that the channel's input symbols are equiprobable. Hence we exploited the area property of EXIT-charts [29] to determine the achievable capacities of the URC-MSDD-aided-DQPSK and IrCC-URC-MSDD-aided-DQPSK systems,

TABLE I: The main parameters of the system

Parameters	Description
R [BPS]	Information rate calculated in Bit Per Symbol (BPS) for all the links in the system
R_c	The code rate of IrCC encoder described in described in Section V-A
K [iteration]	The number of inner iterations described in Section V-A
J [iteration]	The number of outer iterations described in Section V-A
L [bit]	The number of information bits in a frame
M [user]	The number of users in the system
k_1 [frame]	The number of information frames transmitted by each of M users during broadcast phases within a transmission session
k_2 [frame]	The number of parity frames transmitted by each of M users during cooperative phases within a transmission session
G	Original transfer matrix corresponding to the case where all the frames transmitted within a transmission session are successfully decoded
R_{NNCNM}[BPS]	The system's overall information rate
D_{NNCNM}	Diversity order of the system determined by (21)

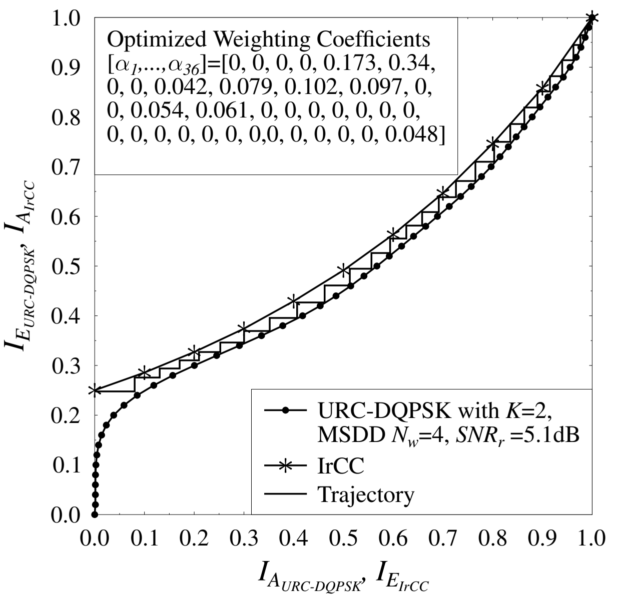

Fig. 3: The EXIT curves of the inner decoder URC-MSDD-aided-DQPSK and the outer decoder IrCC along with the Monte-Carlo simulation based decoding trajectory when $f_d = 0.03$.

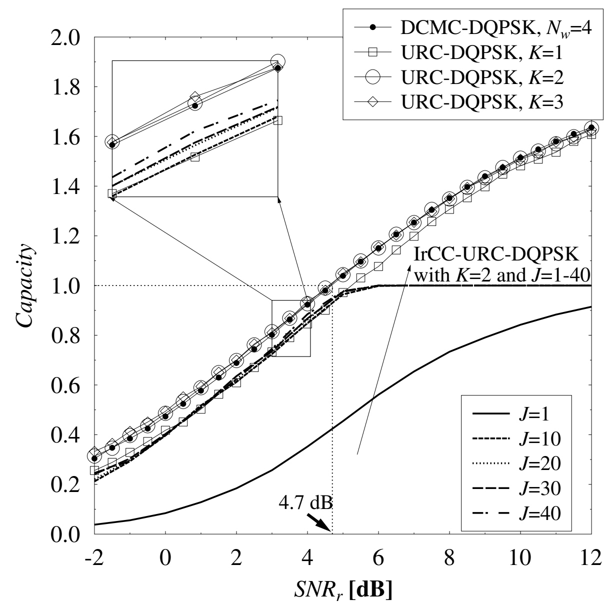

Fig. 4: Channel capacity comparison for the MSDD-aided-DQPSK, URC-MSDD-aided-DQPSK and IrCC-URC-MSDD-aided-DQPSK based systems when $f_d = 0.03$.

which are quantified in Fig. 4. It is seen in Fig. 4 that the capacity curve of the URC-MSDD-aided-DQPSK scheme approaches that of the MSDD-aided-DQPSK arrangement, when $K > 1$ inner iterations [7] are employed for the composite URC-MSDD-aided-DQPSK decoder. It is also demonstrated in Fig. 4 that the attainable capacity improvement becomes negligible for $K > 2$. Therefore, we fix the number of inner iterations to $K = 2$ throughout this paper. The numerical results of Fig. 4 also show that for a sufficiently high number of say $J \geq 30$ outer iterations, the distance between the capacity curve of the IrCC-URC-MSDD-aided-DQPSK scheme and that of the DCMC-MSDD-aided-DQPSK arrangement is less than 0.4 dB. Our simulation results seen in Fig. 5 verify the accuracy of our EXIT chart analysis. When employing $J = 30$ outer iterations[8] between the IrCC and URC components, our IrCC-URC-MSDD-aided-DQPSK channel coding scheme has a vanishingly low BER for SNRs in excess of 5.1 dB, provided that the transmission frame length is sufficiently high. Therefore, we opted for a frame length of $L = 10^6$ bits for our system. At this stage we also define the relaying-aided reduced-distance-related pathloss-reduction. Naturally, this pathloss-reduction becomes unity for each direct source-to-destination link [30].

In the small-scale fading channel, the transmitter can send data at the rate of $R < C|_h$, while maintaining an arbitrarily small error probability, but this idealised performance cannot be maintained for large-scale fading channel [23]. Accordingly, the performance of the proposed IrCC-URC-MSDD-aided-DBPSK(DQPSK) scheme recorded for transmission over the large-scale Rayleigh fading channel is presented in Fig. 6.

[7]The term inner iteration refers to the iterations between the MSDD-aided-MPSK component and the URC decoder, as portrayed in Fig 1.

[8]Outer iterations refer to the iterations between the MSDD-aided-MPSK-URC arrangement and the outer IRCC decoder, as also portrayed in Fig 1.

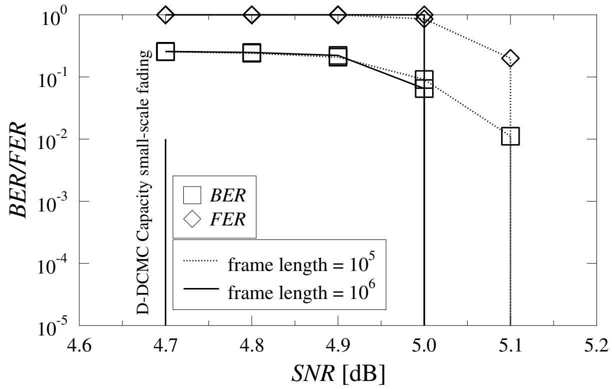

Fig. 5: Performance of the proposed IrCC-URC-MSDD-aided-DQPSK scheme in the small-scale Rayleigh fading channel with $f_d = 0.03$.

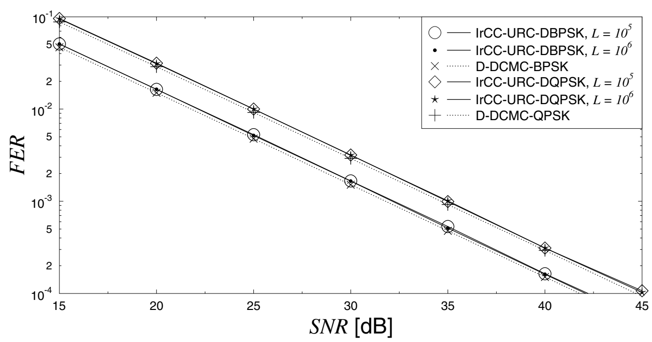

Fig. 6: FER performance of IrCC-URC-MSDD-aided-DBPSK(DQPSK) in large-scale fading channel.

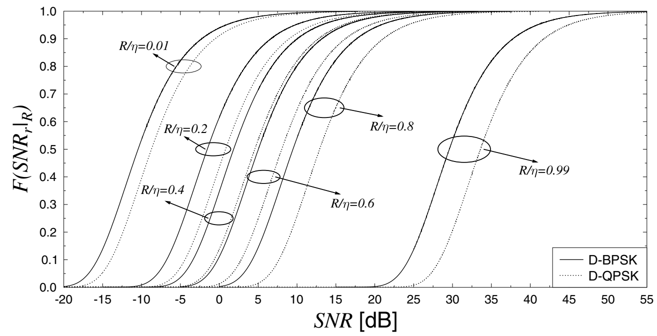

Fig. 7: The complementary cumulative distribution function $F(SNR_r|_R)$.

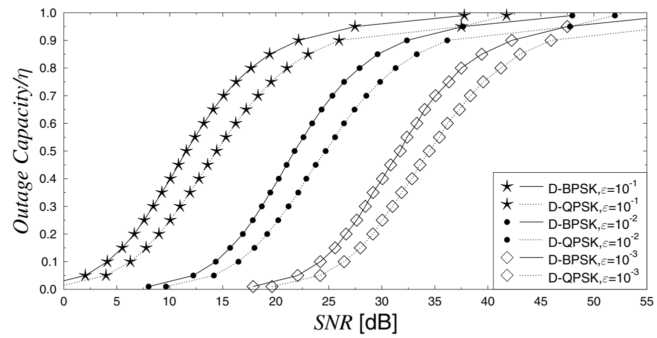

Fig. 8: Outage capacity of D-DCMC for the cases of employing the D-BPSK and the D-QPSK modulation schemes.

B. D-DCMC outage capacity

In the large-scale fading channel, the outage capacity $C_{(\varepsilon)}$ introduced in [23] is defined as the highest possible rate of transmission R, while ensuring that the outage probability P_e remains less than ε. Similar to the formula established for the CCMC case in [23], it can be inferred from (4) that the outage capacity of the D-DCMC channel may be formulated as:

$$C^{D-DCMC}(\varepsilon, \eta) \quad = \quad F^{-1}(1-\varepsilon), \tag{27}$$

where $F(SNR_r|_R)$ is the complementary cumulative distribution function of $|h|^2 = |h_s|^2|h_f|^2$, which is defined as

$$F(SNR_r|_R) \quad = \quad Pr\left\{|h_s|^2 > \frac{SNR_r|_R}{\text{SNR}}\right\}. \tag{28}$$

Note that $F(SNR_r|_R)$ depends on the transmission rate R as well as on the SNR_r, which may be calculated from the corresponding EXIT-chart of a given modulation scheme, namely D-BPSK or D-QPSK. For convenience, the distribution function $F(SNR_r|_R)$ is drawn in Fig. 7 against different values of R/η for both the D-BPSK and D-QPSK scenarios.

Furthermore, the distribution function $F(SNR_r|_R)$ can be used in conjunction with Equation (27) to calculate the outage capacity plotted in Fig. 8 corresponding to different outage probability values ε, namely to $\varepsilon = 10^{-1}, 10^{-2}$ and 10^{-3}. As seen in Fig. 6, the FER performance corresponding to the equivalent outage capacity of both the IrCC-URC-DQPSK and IrCC-URC-DBPSK arrangements is evaluated by calculating the outage capacity corresponding to a given range of outage probability, namely to $\varepsilon = [10^{-1}, 10^{-4}]$. It can also be seen in Fig. 6 that the performance of the IrCC-URC-MSDD-aided-DBPSK scheme as well as that of the IrCC-URC-MSDD-aided-DBPSK scheme transmitting over the large-scale Rayleigh fading channel and recorded for the frame lengths of $L = 10^5, 10^6$ bits is within about 0.4 dB apart from those of the corresponding outage capacity. Since the proposed schemes attain their best performance, when operating in conjunction with a frame length of 10^6 bits, as seen in Fig. 6, we opt for using the frame length of $L = 10^6$ bits for all corresponding results in Section VI.

C. Network Coding Design

Observing the R_{info} expression of (23) and the D_{NNCNM} formula of (21), it becomes plausible that we may conceive different systems having the same network coding rate R_{info}, but different diversity orders of D_{NNCNM} by independently adjusting k_1, k_2 and M. In other words, using (23) and (21), we are able to design a network-coding system having the highest possible diversity order at a given overall normalised data rate of R_{NNCNM}. A higher diversity order implies that the system is capable of achieving an improved FER performance.

In order to employ the generic design principles mentioned above, let us now consider a specific $\boldsymbol{G}_{2\times 4}$-based system and a $\boldsymbol{G}_{4\times 8}$-based design example. The matrix $\boldsymbol{G}_{2\times 4}$ is given in (12), and $\boldsymbol{G}_{4\times 8}$ was provided by [9], [10]:

$$\boldsymbol{G}_{4\times 8} = \left[\begin{array}{cccc|cccc} 1 & 0 & 0 & 0 & 3 & 7 & 3 & 6 \\ 0 & 1 & 0 & 0 & 5 & 7 & 7 & 4 \\ 0 & 0 & 1 & 0 & 2 & 4 & 6 & 1 \\ 0 & 0 & 0 & 1 & 5 & 5 & 3 & 2 \end{array}\right]. \tag{29}$$

Accordingly, the chosen parameters of the $\boldsymbol{G}_{2\times 4}$-based system and those of the the $\boldsymbol{G}_{4\times 8}$-based one are listed in Table II.

It is shown in Table II that the two systems are comparable in terms of having the same parameter values of $R = \{0.5, 1.0\}$, $M = 2$ and $R_{info} = 0.5$. However, the more complex transfer matrix $\boldsymbol{G}_{4\times 8}$ has a higher diversity order of $4 \leq D_{4\times 8} \leq 5$ (as opposed to $3 \leq D_{2\times 4} \leq 3$), hence it is associated with a better detection reliability, but may impose a higher detection complexity at the BS.

It was shown in [4] that the PRBM always suggests a superior performance in comparison to the actual performance obtained by simulations, as also demonstrated by the specific example of Section II-D. According to the analysis presented in Section II-D and Section II-E, since the PALEM can provide the same NNCNM system's performance as that evaluated by the actual simulations, the results on the system's performance in Section VI will be evaluated by using the actual simulations (SIMUL) and PALEM, rather than using PRBM.

Furthermore, by combining the results of the channel coding design presented in Fig 6, the bounds of the system's outage probability can be further exploited in order to estimate the approximate performance of the NNCNM system without Monte-Carlo simulations, which would be very time-consuming.

D. Adaptive Network Coding

The general philosophy of the Diversity versus Multiplexing Trade-off (DMT) is that the specific trade-off would rely on the particular channel conditions that the system experiences [31], [32]. When experiencing sufficiently high quality channels, the multiplexing gain of the system can be increased for example by reducing a number of the PFs transmitted. By contrast, an increased diversity may be achieved by increasing the number of PFs, when the channel conditions degrade [22]. Furthermore, another mechanism may be invoked for the channel coding scheme, namely a channel coding scheme having a higher information rate R may be employed, when a good channel condition is encountered. This results in employing an adaptive channel coding scheme, which was also invoked in [33]. We set aside the investigation of the latter regime for our future work.

In our system, we have opted for further developing this adaptive feedback based solution for the proposed near-capacity channel code. Accordingly, we can increase R_{info} by reducing the number of parity frames transmitted. For example, no further PFs are required, when all the IFs were successfully received during the BPs. More specifically, let us denote the number of PFs transmitted by each user in a transmission session by $k_{2,a}$. In order to increase the achievable multiplexing gain without compromising the diversity gain, it was suggested in [22] that the value of $k_{2,a}$ has to be adaptively changed in each transmission session as follows:

$$k_{2,a} = \begin{cases} 0 & : \text{ If } \Delta = 1 \\ k_2 & : \text{ Otherwise} \end{cases}, \tag{30}$$

where the feedback flag Δ is an acknowledgement bit transmitted by the BS to indicate the successful/unsuccessful receptions of all the Mk_1 IFs transmitted by all M users during their broadcast phases. The value of Δ obeys the following rule:

$$\Delta = \begin{cases} 1 & : \text{ All the } Mk_1 \text{ IFs successfully decoded} \\ 0 & : \text{ Otherwise} \end{cases}. \tag{31}$$

As a result of applying the adaptive feedback-flag based mechanism, the adaptive network code rate $R_{info,adaptive}$ can be calculated as

$$\begin{aligned} R_{info,adaptive} &= \frac{E[\text{Number of transmitted IFs/session}]}{E[\text{Number of all transmitted frames/session}]}, \\ &= \frac{Mk_1}{Mk_1 + E[\Sigma_{j=1}^{M} k_{2,j}]}. \end{aligned} \tag{32}$$

As seen in Fig. 9 displaying the adaptive network coding rate calculated from (32), at a given SNR value, different effective network coding rates are exhibited when different modulation schemes, namely IrCC-URC-DBPSK and IrCC-URC-DQPSK, are employed in our system. Furthermore, the value of the adaptive network coding rate approaches $R_{info,adaptive} = 1$, when the SNR is increased. This can be inferred from (23) and (32) by bearing in mind that the maximum value of the adaptive system's overall rate can be calculated as

$$\begin{aligned} \text{Max}\{R_{NNCNM,adaptive}\} &= \text{Max}\{R_{info,adaptive}R\}, \\ &= \text{Max}\left\{\frac{Mk_1R}{Mk_1 + E[\Sigma_{j=1}^{M} k_{2,j}]}\right\}, \\ &= R, \end{aligned} \tag{33}$$

when the value of $E[\Sigma_{j=1}^{M} k_{2,j}]$ approaches $E[\Sigma_{j=1}^{M} k_{2,j}] = 0$. The condition of $E[\Sigma_{j=1}^{M} k_{2,j}] = 0$ would hold when no further PFs are required to be transmitted to the BS. Accordingly, it can be readily shown from (23) and (33) that the maximum value ϱ of the E_b/N_0-improvement obtained by employing the adaptive mechanism may be formulated as

$$\begin{aligned} \varrho &= \text{Max}\left\{10\log\left(\frac{R_{NNCNM,adaptive}}{R_{NNCNM}}\right)\right\} [\text{dB}], \\ &= 10\log\left(\frac{k_1+k_2}{k_1}\right) [\text{dB}], \end{aligned} \tag{34}$$

where the system's overall rate $R_{NNCNM} = \frac{k_1R}{k_1+k_2}$ is given in (23). As a result, the maximum value is $\varrho = 3$ dB in our configurations, where we have either $k_1 = k_2 = 1$ or $k_1 = k_2 = 2$.

VI. Numerical Results and Discussions

Observe in Fig. 10 and Fig 11 that the system's actual FER performance curves are always between their upper bound and lower bound. Thus, the upper and lower bounds may be used to estimate the performance of other NNCNM systems, which have a performance determined by extremely long simulations, when a large transfer matrix is employed.

As seen in Fig. 12, the system's performance suggested by both the Monte-Carlo simulations and PALEM is identical,

TABLE II: The main parameters of the NNCNM systems based on the $\boldsymbol{G}_{2\times4}$ and $\boldsymbol{G}_{4\times8}$.

Parameters	$\boldsymbol{G}_{2\times4}$ **system**	$\boldsymbol{G}_{4\times8}$ **system**
R[BPS]	1.0 (DQPSK), 0.5 (DBPSK)	1.0 (DQPSK), 0.5 (DBPSK)
R_c	0.5	0.5
K [iteration]	2	2
J [iteration]	30	30
L [bit]	10^6	10^6
M [user]	2	2
k_1 [frame]	1	2
k_2 [frame]	1	2
$\boldsymbol{G}$	$\boldsymbol{G}_{2\times4}$	$\boldsymbol{G}_{4\times8}$
R_{NNCNM} [BPS]	0.5 (DQPSK), 0.25 (DBPSK)	0.5 (DQPSK), 0.25 (DBPSK)
D_{NNCNM}	$3 \leq D_{2\times4} \leq 3$	$4 \leq D_{4\times8} \leq 5$

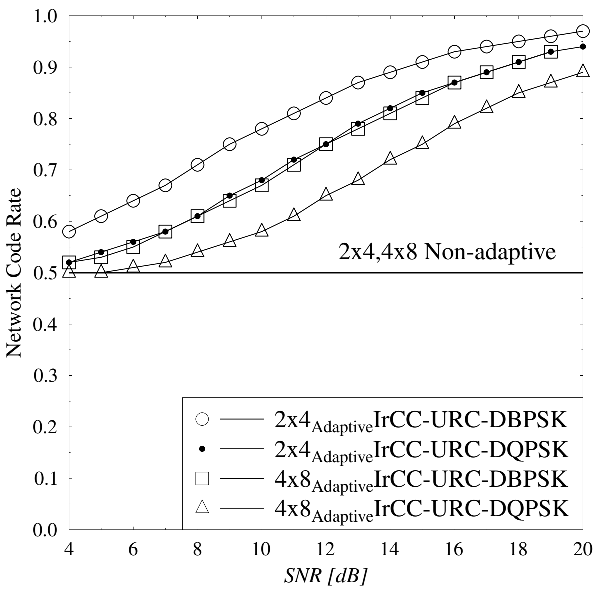

Fig. 9: Network coding rate when the adaptive mechanism is applied in the system.

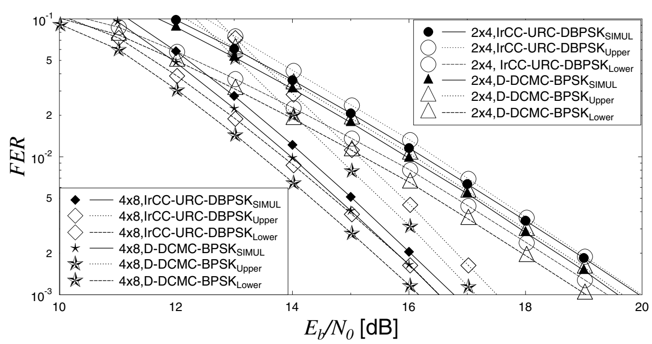

Fig. 10: FER performance comparison between $\boldsymbol{G}_{2\times4}$ and $\boldsymbol{G}_{4\times8}$ based systems employing the IrCC-URC-MSDD-aided-DBPSK scheme and idealised/perfect D-DCMC-BPSK channel coding schemes and their corresponding bounds.

which validates the analysis presented in Section II-D and Section II-E. As a result, the less complex PALEM may be used to replace the Monte-Carlo simulations in evaluating the NNCNM system's performance. Moreover, in line with the common logic, the more complex NNCNM system employing the IrCC-URC-MSDD-aided-DQPSK FEC scheme exhibits

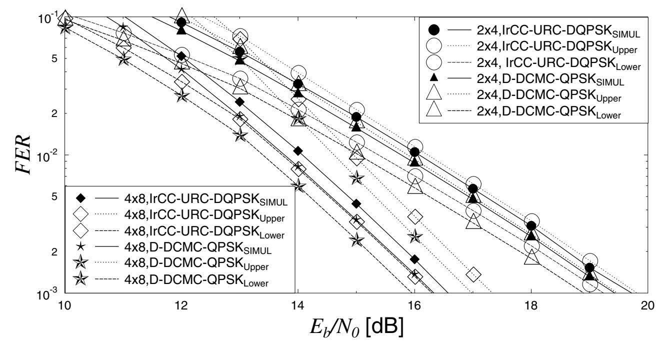

Fig. 11: FER performance comparison between $\boldsymbol{G}_{2\times4}$ and $\boldsymbol{G}_{4\times8}$ based systems employing the IrCC-URC-MSDD-aided-DQPSK scheme and idealised/perfect D-DCMC-QPSK channel coding schemes and their corresponding bounds.

a slightly better performance for both the $\boldsymbol{G}_{4\times8}$ and $G_{2\times4}$ scenarios in comparison to those of the NNCNM system using the IrCC-URC-MSDD-aided-DBPSK FEC scheme as seen in Fig. 12.

It can be seen from Fig. 10, Fig. 11 and Fig. 12 that the difference in the diversity order of the $\boldsymbol{G}_{2\times4}$ and $\boldsymbol{G}_{4\times8}$ based systems, as specified in Section V-C, is reflected by the different slope of the performance curves. As a benefit, the $\boldsymbol{G}_{4\times8}$-based system outperforms the $\boldsymbol{G}_{2\times4}$-based arrangement by about 3.1 dB to 3.3 dB at an FER of 10^{-3} in the scenarios of using the D-DCMC as well as the IrCC-URC-DBPSK and IrCC-URC-DQPSK channel coding schemes.

Another important result gleaned from both Fig. 10 and Fig. 11 is that the performance of the NNCNM systems using the idealised/perfect D-DCMC channel coding schemes represents the best-case performance bound of all NNCNM systems using realistic channel coding schemes, provided that those schemes employ the same modulation scheme as well as have the same equivalent data rate R.

Fig. 10 and Fig. 11 show the significant FERvsE$_b$N$_0$-performance improvement of 18.0 dB to 19.0 dB at a FER of 10^{-3} brought about by the employment of network coding, when comparing the performance of the $\boldsymbol{G}_{4\times8}$ based systems to the corresponding single-link performance using the same coding schemes. It can also be seen in Fig. 10 (Fig. 11) that the performance of the $\boldsymbol{G}_{4\times8}$ and $\boldsymbol{G}_{2\times4}$-based systems using our IrCC-URC-MSDD-aided-DBPSK(DQPSK) FEC scheme was within 0.3 dB to 0.5 dB from that of the corresponding systems relying on the assumption of using an idealised/perfect D-

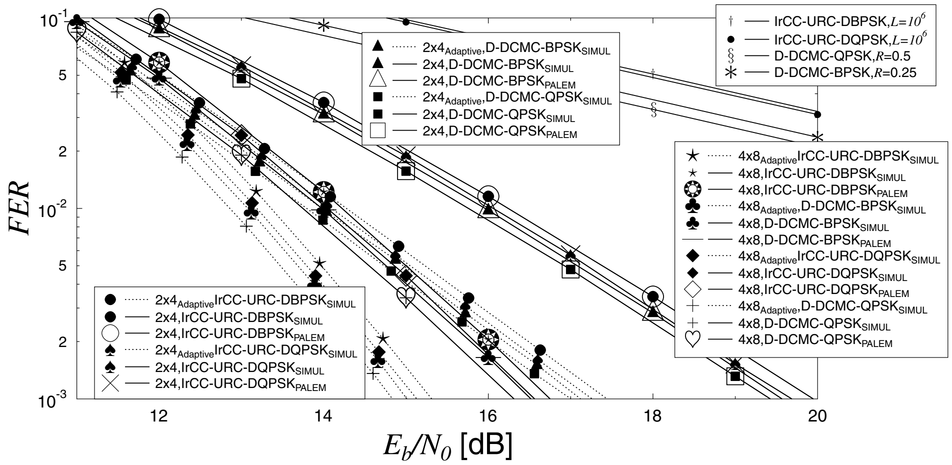

Fig. 12: FER performance comparison between $\boldsymbol{G}_{2\times4}$/$\boldsymbol{G}_{2\times4,\text{Adaptive}}$ and $\boldsymbol{G}_{4\times8}$/$\boldsymbol{G}_{4\times8,\text{Adaptive}}$ based systems employing the IrCC-URC-MSDD-aided-DMPSK scheme and idealised/perfect D-DCMC-MPSK channel coding schemes along with the corresponding the single link performance.

DCMC-BPSK(QPSK) capacity-achieving FEC channel coding scheme. In addtion, as seen in Fig. 12, the performance curves of the adaptive systems employing ideal/perfect coding operating exactly at the D-DCMC-BPSK(QPSK) also exhibit a distance of 0.3 dB to 0.5 dB from the curves characterising the performance of the adaptive $\boldsymbol{G}_{2\times4}$ and $\boldsymbol{G}_{4\times8}$ based systems employing the realistic IrCC-URC-MSDD-aided-DBPSK(DQPSK) coding scheme.

As expected, it can be seen in Fig. 12 that the adaptive feedback-flag based mechanism of (30) provides a significant E_b/N_0-performance improvement in comparison to that of the system operating without the adaptive mechanism. The attainable E_b/N_0-improvement increases upon increasing E_b/N_0. More specifically, an E_b/N_0-performance improvement of 1.4 dB and 2.5 dB is recorded at an $FER = 10^{-3}$ when applying the adaptive feedback-flag based mechanism for the $\boldsymbol{G}_{4\times8}$-based and for the $\boldsymbol{G}_{2\times4}$-based system, respectively. Upon increasing the E_b/N_0, this improvement approaches its maximum value of $\varrho = 3$ dB, as suggested by our analysis in Section V-D.

VII. Conclusions

In this contribution, we investigated new Near-capacity Non-coherent Cooperative Network-coding aided Multi-user (NNCNM) systems using our IrCC-URC-MSDD-aided-DMPSK scheme. The achievable performance was benchmarked against the corresponding systems employing the idealised/perfect capacity-achieving FEC schemes assumed to be operating exactly at the D-DCMC capacities. EXIT charts were used to assist the design of NNCNM systems as well as to compute the benchmarked D-DCMC-outage capacity. We also derived the bounds of the NNCNM performance for the sake of designing network coding. The less complex technique referred to as the Pragmatic Algebraic Linear Equation Method (PALEM) was proposed to replace the Monte-Carlo simulation. The performance of our proposed schemes was within 0.3-0.5 dB from that of the corresponding systems relying on the assumption of using an idealised/perfect D-DCMC-BPSK(QPSK) capacity-achieving FEC scheme. We considered the joint treatment of channel and network coding, leading to a multiplexing gain, which has a maximum of $\varrho = 10\log(\frac{k_1+k_2}{k_1})$ dB, i.e $\varrho = 3$ dB in the configurations considered.

References

[1] H. V. Nguyen, C. Xu, S. X. Ng, J. L. Rebelatto, Y. Li, and L. Hanzo, "Near-capacity non-coherent network-coding aided scheme for cooperative multi-user communications," in *Proc. 2011 IEEE Veh. Technol. Conf. – Fall*, pp. 1–5.

[2] R. Ahlswede, N. Cai, S.-Y. Li, and R. Yeung, "Network information flow," *IEEE Trans. Inf. Theory*, vol. 46, pp. 1204–1216, July 2000.

[3] A. Asterjadhi, E. Fasolo, M. Rossi, J. Widmer, and M. Zorzi, "Toward network coding-based protocols for data broadcasting in wireless ad hoc networks," *IEEE Trans. Wireless Commun.*, vol. 9, pp. 662–673, Feb. 2010.

[4] H. V. Nguyen, S. X. Ng, and L. Hanzo, "Performance bounds of network coding aided cooperative multiuser systems," *IEEE Signal Process. Lett.*, vol. 18, pp. 435–438, July 2011.

[5] M. Xiao and T. Aulin, "Optimal decoding and performance analysis of a noisy channel network with network coding," *IEEE Trans. Commun.*, vol. 57, pp. 1402–1412, May 2009.

[6] M. Xiao and M. Skoglund, "M-user cooperative wireless communications based on nonbinary network codes," in *Proc. 2009 IEEE Inf. Theory Workshop Netw. Inf. Theory*, pp. 316–320.

[7] M. Xiao and M. Skoglund, "Design of network codes for multiple-user multiple-relay wireless networks," in *Proc. 2009 IEEE International Symp. Inf. Theory*, pp. 2562–2566.

[8] M. Xiao and M. Skoglund, "Multiple-user cooperative communications based on linear network coding," *IEEE Trans. Commun.*, Dec. 2010.

[9] J. L. Rebelatto, B. F. Uchôa-Filho, Y. Li, and B. Vucetic, "Generalized distributed network coding based on nonbinary linear block codes for multi-user cooperative communications," in *Proc. 2010 IEEE International Symp. Inf. Theory*, pp. 943–947.

[10] J. Rebelatto, B. Uchoa Filho, Y. Li, and B. Vucetic, "Multi-user cooperative diversity through network coding based on classical coding theory," *IEEE Trans. Signal Process.*, vol. PP, no. 99, p. 1, 2011.

[11] M. Tücher and J. Hagenauer, "Exit charts of irregular codes," in *Proc. 2002 Conf. Inf. Sciences Syst. [CDROM]*.

[12] M. Tuchler, "Design of serially concatenated systems depending on the block length," *IEEE Trans. Commun.*, vol. 52, pp. 209–218, Feb. 2004.

[13] S. ten Brink, "Convergence behavior of iteratively decoded parallel concatenated codes," *IEEE Trans. Commun.*, vol. 49, pp. 1727–1737, Oct. 2001.

[14] C. Xu, S. X. Ng, and L. Hanzo, "Near-capacity irregular convolutional coded cooperative differential linear dispersion codes using multiple-symbol differential detection," *IEEE Signal Process. Lett.*, vol. 18, pp. 173–176, Mar. 2011.

[15] P. Ho and D. Fung, "Error performance of multiple-symbol differential detection of PSK signals transmitted over correlated Rayleigh fading channels," *IEEE Trans. Commun.*, vol. 40, pp. 1566–1569, Oct. 1992.

[16] V. Pauli, L. Lampe, and R. Schober, " 'Turbo DPSK' using soft multiple-symbol differential sphere decoding," *IEEE Trans. Inf. Theory*, vol. 52, pp. 1385–1398, Apr. 2006.

[17] L. Bahl, J. Cocke, F. Jelinek, and J. Raviv, "Optimal decoding of linear codes for minimizing symbol error rate," *IEEE Trans. Inf. Theory*, vol. 20, pp. 284–287, Mar 1974.

[18] S. X. Ng, J. Wang, M. Tao, L.-L. Yang, and L. Hanzo, "Iteratively decoded variable length space-time coded modulation: code construction and convergence analysis," *IEEE Trans. Wireless Commun.*, vol. 6, pp. 1953–1963, May 2007.

[19] R. Tee, T. Nguyen, S. Ng, L.-L. Yang, and L. Hanzo, "Luby transform coding aided bit-interleaved coded modulation for the wireless internet," in *Proc. 2007 IEEE Veh. Technol. Conf. – Fall*, pp. 2025–2029.

[20] T. Nguyen, M. El-Hajjar, L. Yang, and L. Hanzo, "A systematic Luby transform coded V-BLAST system," in *Proc. 2008 IEEE International Conf. Commun.*, pp. 775–779.

[21] O. Iscan and C. Hausl, "Iterative network and channel decoding for the relay channel with multiple sources," in *Proc. 2011 IEEE Veh. Technol. Conf. – Fall)*, pp. 1–5.

[22] J. Rebelatto, B. Uchoa-Filho, Y. Li, and B. Vucetic, "Adaptive distributed network-channel coding," *IEEE Trans. Wireless Commun.*, vol. 10, pp. 2818–2822, Sep. 2011.

[23] D. Tse and P. Viswanath, *Fundamentals of Wireless Communications*. Cambridge University Press, 2005.

[24] C. F. Golub and G. H. Van Loan, *Matrix Computations*. Johns Hopkins Studies in Mathematical Sciences: Johns Hopkins University Press, 1996.

[25] J. Laneman, D. Tse, and G. Wornell, "Cooperative diversity in wireless networks: efficient protocols and outage behavior," *IEEE Trans. Inf. Theory*, vol. 50, pp. 3062–3080, Dec. 2004.

[26] SAGE, "Open source mathematics software." Available: http://wwwsagemath.org/.

[27] L. Kong, S. X. Ng, R. Tee, R. Maunder, and L. Hanzo, "Reduced-complexity near-capacity downlink iteratively decoded generalized multi-layer space-time coding using irregular convolutional codes," *IEEE Trans. Wireless Commun.*, vol. 9, pp. 684–695, Feb. 2010.

[28] L. Hanzo, T. Liew, B. Yeap, R. Tee, and S. Ng, *Turbo Coding, Turbo Equalisation and Space-Time Coding (EXIT-Chart-Aided Near-Capacity Designs for Wireless Channels)*. Wiley-IEEE Press, 2011.

[29] A. Ashikhmin, G. Kramer, and S. ten Brink, "Extrinsic information transfer functions: model and erasure channel properties," *IEEE Trans. Inf. Theory*, vol. 50, pp. 2657–2673, Nov. 2004.

[30] H. Ochiai, P. Mitran, and V. Tarokh, "Design and analysis of collaborative diversity protocols for wireless sensor networks," in *Proc. 2004 IEEE Veh. Technol. Conf. – Fall*, vol. 7, pp. 4645–4649.

[31] A. Goldsmith and S.-G. Chua, "Adaptive coded modulation for fading channels," *IEEE Trans. Commun.*, vol. 46, pp. 595–602, May 1998.

[32] C. Wong and L. Hanzo, "Upper-bound performance of a wide-band adaptive modem," *IEEE Trans. Commun.*, vol. 48, pp. 367–369, Mar. 2000.

[33] S. X. Ng, C. Qian, D. Liang, and L. Hanzo, "Adaptive turbo trellis coded modulation aided distributed space-time trellis coding for cooperative communications," in *Proc. 2010 IEEE Veh. Technol. Conf. – Spring)*, pp. 1–5.

Hung Viet Nguyen received the B.Eng. degree in Electronics & Telecommunications from Hanoi University of Science and Technology (HUST), Hanoi, Vietnam, in 1999 and his M.Eng. in Telecommunications from Asian Institute of Technology (AIT), Bangkok, Thailand, in 2002. He is currently working towards the Ph.D. degree in the Communications Group, School of Electronics and Computer Science, University of Southampton, Southampton, UK. He is involved in the European Union project known as OPTIMIX. His research interests include cooperative communications, channel coding and network coding.

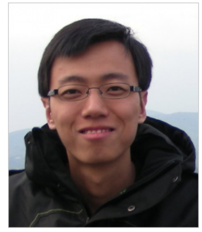

Chao Xu received a B.Eng. degree from Beijing University of Posts and Telecommunications, Beijing, China, and a BSc(Eng) with First Class Honours from Queen Mary, University of London, London, UK, through a Sino-UK joint degree program in 2008, both in Telecommunications Enginneering with Management. In 2009, he obtained a MSc degree with distinction in radio frequency communication systems from the University of Southampton, Southampton, UK, and he was awarded IEEE Communications Society UK&RI Chapter Best MSc Student in Broadband and Mobile Communication Networks. He is currently working towards the PhD degree with the Research Group of Communications, Signal Processing and Control, School of Electronics and Computer Science, University of Southampton, UK. His research interests include reduced-complexity MIMO design, non-coherent space-time modulation detection, EXIT-chart-aided turbo detection as well as cooperative communications.

Dr Soon Xin Ng (S'99-M'03-SM'08) received the B.Eng. degree (First class) in electronics engineering and the Ph.D. degree in wireless communications from the University of Southampton, Southampton, U.K., in 1999 and 2002, respectively. From 2003 to 2006, he was a postdoctoral research fellow working on collaborative European research projects known as SCOUT, NEWCOM and PHOENIX. Since August 2006, he has been a member of academic staff in the School of Electronics and Computer Science, University of Southampton. He is involved in the OPTIMIX and CONCERTO European projects as well as the IU-ATC and UC4G projects. He is currently a senior lecturer at the University of Southampton. His research interests include adaptive coded modulation, coded modulation, channel coding, space-time coding, joint source and channel coding, iterative detection, OFDM, MIMO, cooperative communications, distributed coding and quantum error correction codes. He has published over 140 papers and co-authored two John Wiley/IEEE Press books in this field. He is a senior member of the IEEE, a Chartered Engineer and a fellow of the Higher Education Academy in the UK.

Lajos Hanzo FREng, FIEEE, FIET, Fellow of EURASIP, DSc received his degree in electronics in 1976 and his doctorate in 1983. In 2009 he was awarded the honorary doctorate "Doctor Honoris Causa" by the Technical University of Budapest. During his 35-year career in telecommunications he has held various research and academic posts in Hungary, Germany and the UK. Since 1986 he has been with the School of Electronics and Computer Science, University of Southampton, UK, where he holds the chair in telecommunications. He has successfully supervised about 80 PhD students, co-authored 20 John Wiley/IEEE Press books on mobile radio communications totalling in excess of 10,000 pages, published 1250+ research entries at IEEE Xplore, acted both as TPC and General Chair of IEEE conferences, presented keynote lectures and has been awarded a number of distinctions. Currently he is directing an academic research team, working on a range of research projects in the field of wireless multimedia communications sponsored by industry, the Engineering and Physical Sciences Research Council (EPSRC) UK, the European IST Programme and the Mobile Virtual Centre of Excellence (VCE), UK. He is an enthusiastic supporter of industrial and academic liaison and he offers a range of industrial courses. He is also a Governor of the IEEE VTS. Since 2008 he has been the Editor-in-Chief of the IEEE Press and since 2009 a Chaired Professor also at Tsinghua University, Beijing. For further information on research in progress and associated publications please refer to http://www-mobile.ecs.soton.ac.uk